

Mitochondrial dysfunction in the pathogenesis of Ullrich congenital muscular dystrophy and prospective therapy with cyclosporins

Alessia Angelin, Tania Tiepolo, Patrizia Sabatelli, Paolo Grumati, Natascha Bergamin, Cristina Golfieri, Elisabetta Mattioli, Francesca Gualandi, Alessandra Ferlini, Luciano Merlini, Nadir M. Maraldi, Paolo Bonaldo, and Paolo Bernardi

PNAS published online Jan 10, 2007;
doi:10.1073/pnas.0610270104

This information is current as of January 2007.

E-mail Alerts	This article has been cited by other articles: www.pnas.org#otherarticles
Rights & Permissions	Receive free email alerts when new articles cite this article - sign up in the box at the top right corner of the article or click here .
Reprints	To reproduce this article in part (figures, tables) or in entirety, see: www.pnas.org/misc/rightperm.shtml
	To order reprints, see: www.pnas.org/misc/reprints.shtml

Notes:

Table 1. Clinical and genetic characteristics of patients

Patient	Age	Phenotype	Collagen VI	Mutation
1	23	Floppy at birth. First steps at 13 months. Limb girdle wasting and weakness, multiple joint contractures, and distal laxity.	Mild reduction in muscle and fibroblasts	<i>COL6A3</i> homozygous nonsense Arg465Stop mutation (ref. 10)
2	6	Floppy at birth with talus of the feet. Never able to stand or walk. Diffuse muscle wasting and weakness, contractures, and distal laxity.	Marked reduction in muscle	<i>COL6A1</i> <i>de novo</i> heterozygous del15921–935 mutation
3	3	Floppy at birth. Congenital hip dislocation. Never able to walk. Diffuse muscle wasting and weakness, contractures, and distal laxity.	Marked reduction in muscle	Not known
4	9	Floppy at birth. Able to stand with support. Diffuse muscle wasting and weakness. Spine thoracic kyphosis, keloid formation, proximal contractures, and distal laxity.	Mild reduction in muscle and fibroblasts	<i>COL6A1</i> <i>de novo</i> heterozygous Gly284Arg mutation
5	11	Floppy at birth. Congenital hip dislocation; only seated. Diffuse muscle weakness, scoliosis, diffuse contractures, and distal laxity.	Absent in muscle fibres and fibroblasts	<i>COL6A1</i> homozygous delG1456 mutation (ref. 14)

All patients listed experienced onset of muscle weakness at birth. Patient 5 was the only patient listed who required mechanical ventilation, at 11 years of age, and became the only patient to have died, also at 11 years of age.

VI ranged from mild (patients 1 and 4) to marked reduction (patients 2 and 3) to complete absence (patient 5). Patients 1 and 5 had genetically proven UCMD (10, 14), whereas the mutation of patients 2 and 4 is identified here (see *Materials and Methods*). Genetic analysis was not available for patient 3, who presented the typical clinical and immunohistochemical features of UCMD. The mutation affected the *COL6A1* gene in three cases (patients 2, 4, and 5) and the *COL6A3* gene in one case (patient 1) and was undefined in one case (patient 3).

We studied the occurrence of apoptosis in biopsies from quadriceps muscle. When compared with that of a healthy donor, the frequency of apoptotic nuclei was much higher in all of the UCMD samples, with values ranging between an \approx 10-fold increase for patients 1, 2, and 3 to a $>$ 300-fold increase for patient 5 (Fig. 1A). Two biopsies were available for patient 4, taken at 4 and 9 years of age. Interestingly, the incidence of apoptosis was always much higher than that observed in cultures from the healthy donor, yet the frequency decreased by 1 order of magnitude between the two measurements. This important finding indicates that the occurrence of apoptosis is variable in the course of the disease and probably explains why there is no quantitative match between increased apoptosis and reduced collagen VI expression in the muscle biopsies of UCMD patients, as revealed by a selective antibody against collagen VI (Fig. 1B). Reduced labeling of collagen VI was always prominent at the level of basal lamina, as documented by the absence of colocalization with perlecan, whereas the protein was still detectable in the extracellular matrix in perivascular fibrotic regions between muscle fibers (Fig. 1C). These findings suggest that the critical factor for development of muscular dystrophy is the selective deficiency of collagen VI in the endomysium.

To experimentally test the existence of a causal link between the lack of collagen VI and apoptosis, we established muscle cell cultures from the biopsies and studied the occurrence of apoptosis after plating them on plastic or collagen VI. We found that the cultures from all patients displayed a higher incidence of apoptosis compared with those from healthy donors and that plating on collagen VI or treatment with CsA fully normalized the occurrence of apoptosis in the patient samples (Fig. 2A). Cultures from patients 2, 3, and 4 displayed low levels of collagen VI (Fig. 2B) as expected and as already had been shown for patient 1 (10), whereas collagen VI was completely absent in cell cultures obtained from patient 5 (14).

We next studied mitochondrial function in living muscle cell cultures to assess whether the antiapoptotic effects of collagen VI and CsA could be traced to mitochondria. As expected, addition of the F_1F_0 ATP synthase inhibitor oligomycin to cultures established from the healthy donors did not cause mitochondrial depolariza-

tion, which was instead promptly elicited by the addition of the protonophore carbonyl cyanide *p*-trifluoromethoxyphenylhydrazone (FCCP) (Fig. 3A and A'). The addition of oligomycin was instead followed by mitochondrial depolarization in the cells from all UCMD patients, although only the results from patients 1 and 2 are shown for clarity (open symbols in Fig. 3B, B', C, and C'). Remarkably, the response to oligomycin was fully normalized by treatment with CsA (filled symbols in Fig. 3B and B') or with the intracellular Ca^{2+} chelator 1,2-bis(2-aminophenoxy)ethane-*N,N,N',N'*-tetraacetic acid tetraacetoxymethyl ester (filled symbols in Fig. 3C and C') or by plating cells on collagen VI (Fig. 3D and D'), suggesting an involvement of the PTP in the pathogenesis of UCMD. These findings suggest that cells from UCMD patients have a latent mitochondrial dysfunction that can be selectively amplified by oligomycin, as has been shown previously for the mouse model of collagen VI deficiency (12).

The muscle cell cultures established from healthy donors and from patients 1–3 were further studied by using electron microscopy (Fig. 4). In the UCMD samples, the mitochondrial area/perimeter ratio was significantly increased to attain values 62.5%, 75%, and 50% higher than those of healthy donors for patients 1, 2, and 3, respectively ($P < 0.05$). This finding indicates that, in UCMD muscle cells, mitochondria are significantly less elongated than in normal samples. We also found that 4–8% of mitochondria of patients had an increased short axis value ($>$ 400 nm) compared with control ($<$ 300 nm). Taken together, these findings suggest the presence of a fraction of mitochondria with increased size in UCMD cells. A small percentage of cells from UCMD patients (between 4% and 5%, compared with 1% for cells from healthy donors) also displayed swollen mitochondria, with hypodense matrix and absence of cristae (Fig. 4). Remarkably, when the UCMD cells were plated on collagen VI, the mitochondrial area/perimeter ratio and short axis values became similar to those of healthy donors (Fig. 4E), and plating on collagen VI or treatment with CsA decreased the numbers of cells with swollen mitochondria to those observed in cultures from healthy donors (Fig. 5B). Treatment of cultures with oligomycin increased the percentage of cells with swollen mitochondria to 4% in control and to $>$ 40% in UCMD patients (Fig. 5). The effect of oligomycin could be prevented by treatment with CsA, and the percentages of cells bearing swollen mitochondria were restored to values similar to basal in all cell cultures (Fig. 5B).

To sort the inhibitory effects of CsA on the PTP from those on calcineurin (15), we studied the effects of methylAla³ethylVal⁴-cyclosporin (also called Debio 025), a nonimmunosuppressive cyclosporin where sarcosine in position 3 and methyl leucine in position 4 of CsA are replaced by

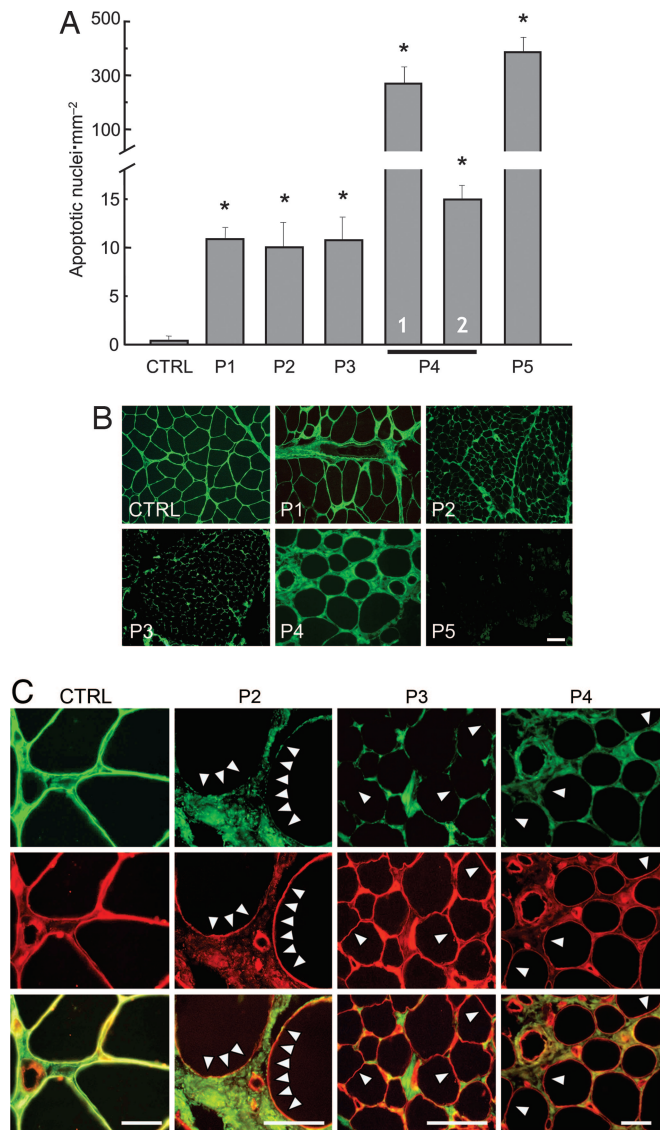


Fig. 1. Incidence of apoptosis and expression of collagen VI in muscle biopsies from a healthy donor and UCMD patients. (A) Biopsies from a healthy donor (CTRL) and five UCMD patients (P1–P5) were scored for the presence of apoptotic nuclei with the TUNEL reaction. For patient 4, columns 1 and 2 refer to biopsies taken at 4 and 9 years of age, respectively. *, $P < 0.01$ for each patient vs. healthy donor. (B) Muscle biopsies from a healthy donor (CTRL) and five UCMD patients (P1–P5) were studied by immunofluorescence for collagen VI. (Scale bar, 20 μm .) (C) Muscle biopsies from a healthy donor (CTRL) and three UCMD patients (P2–P4) were studied by immunofluorescence for collagen VI (COLVI, green fluorescence) (Top) and perlecan (red fluorescence) (Middle), and a merge is shown in Bottom. Arrowheads mark examples of a lack of collagen VI staining at the basal lamina. (Scale bars, 20 μm .)

D-methyl alanine and ethyl valine, respectively. This specific cyclophilin inhibitor maintains the inhibitory properties displayed by CsA on the PTP in isolated mitochondria (16) and is more potent than CsA at inhibiting the permeability transition in mice *in vivo* while displaying a total lack of inhibition of calcineurin (L. Nicolosi, E. Palma, M. E. Soriano, A. Rasola, F. Chiara, F. Finetti, G. Vuaginiaux, J.-M. Dumont, C. T. Baldari, and P. Bernardi, unpublished observations). Debio 025 was as effective as CsA at preventing oligomycin-dependent mitochondrial depolarization in cells from UCMD patients (Fig. 6 A and B) and restored the occurrence of apoptosis to the level displayed by cells from a healthy donor (Fig. 6C).

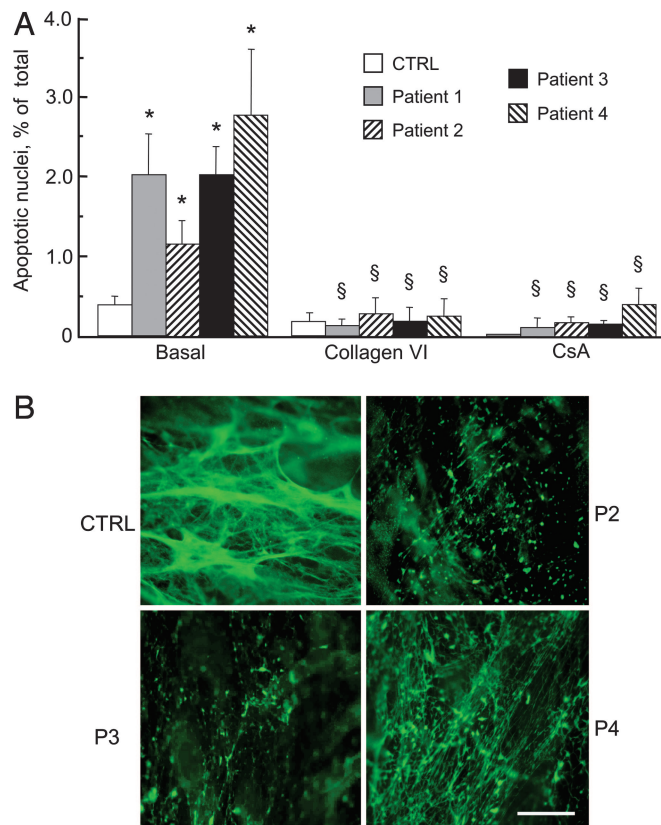


Fig. 2. Incidence of apoptosis and expression of collagen VI in muscle cell cultures from a healthy donor and UCMD patients. (A) Primary myoblast cultures from a healthy donor (CTRL) and four UCMD patients were plated on plastic dishes or on collagen VI and scored for the presence of apoptotic nuclei by the TUNEL reaction. Where indicated, cells plated on plastic dishes were incubated with 1.6 μM CsA for 2 h. Data are the mean of three independent experiments \pm SD. *, $P < 0.01$ for each patient vs. healthy donor; §, not significant for each patient vs. healthy donor. (B) Collagen VI was detected by immunofluorescence in cultured myoblasts from a healthy donor (CTRL) and three UCMD patients (P2–P4). Note that in the healthy donor collagen VI is secreted and organized in a dense fibrillar network, whereas in the UCMD patients collagen VI staining is severely reduced, with residual labeling in the form of small dots. (Scale bar, 20 μm .)

Discussion

Here we have established that patients affected by UCMD show an increased rate of apoptosis in skeletal muscle *in vivo* and in myoblast cultures derived from biopsies. The muscle cell cultures also display a measurable fraction of altered mitochondria, with morphological alterations that range from shape changes to overt swelling. These changes are matched by a latent mitochondrial dysfunction that can be revealed by the addition of the F_1F_0 ATPase inhibitor oligomycin, which caused mitochondrial depolarization only in the cultures from UCMD patients. Oligomycin also dramatically increased the number of swollen mitochondria, this effect being particularly prominent in the cultures from UCMD patients.

Oligomycin is expected to cause hyperpolarization in healthy respiring cells, where the mitochondrial membrane potential is maintained by proton pumping by the respiratory chain and the proton electrochemical gradient is used to drive ATP synthesis (17). The mitochondrial depolarization induced by oligomycin in muscle fibers from *Col6a1*^{-/-} mice (12) and in myoblasts from UCMD patients (this work) is therefore an anomalous response, which suggests that the membrane potential is not maintained by respiration but rather by the mitochondrial ATP synthase working “in reverse” to pump protons from the matrix to the intermembrane

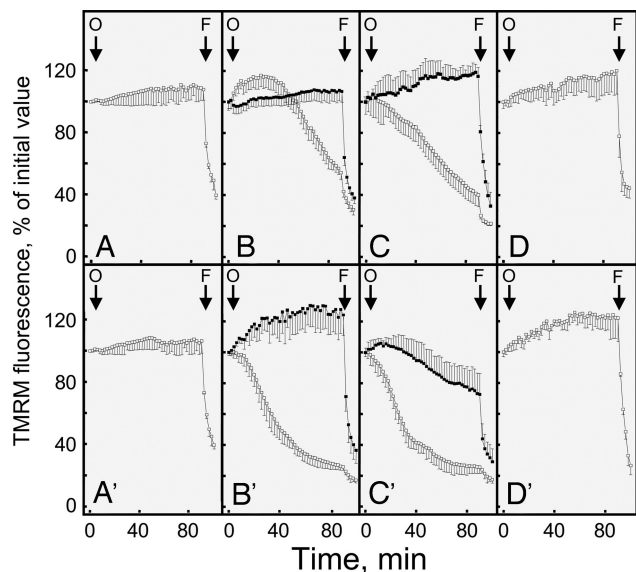


Fig. 3. Changes of mitochondrial TMRM fluorescence induced by oligomycin in muscle cell cultures from a healthy donor and UCMD patients. Myoblasts from two healthy donors (A and A') and from UCMD patients 1 (B–D) and 2 (B'–D') were loaded with TMRM and studied as described in *Materials and Methods*. Cells were seeded on glass (A–C and A'–C') or on collagen VI (D and D'). Where indicated by arrows, 6 μ M oligomycin (O) and 4 μ M carbonyl cyanide *p*-trifluoromethoxyphenylhydrazone (FCCP) (F) were added in the absence of further treatments (open symbols) or after treatment for 30 min with 1.6 μ M CsA or 5 μ M 1,2-bis(2-aminophenoxy)ethane-*N,N,N',N'*-tetraacetic acid tetraacetoxymethyl ester (filled symbols in B and B' and C and C', respectively). Similar results were obtained with cells from patients 3 and 4, and the results shown are representative of at least five repeats per patient.

space, thereby consuming glycolytic ATP. This respiratory deficiency could be due to depletion of pyridine nucleotides and cytochrome *c*, which can be lost via the PTP even in the absence of overt swelling (18–20). Treatment of cultures from UCMD patients with CsA prevented mitochondrial dysfunction and normalized the incidence of apoptosis, indicating that inappropriate opening of the PTP is the basis for both events.

It is remarkable that the mitochondrial defect can be revealed in primary cultures from patients with clinical signs of UCMD, irrespective of whether the primary genetic defect is in the *COL6A1* or *COL6A3* gene. Furthermore, the mitochondrial defect is present both in homozygous (patient 1) and in heterozygous (patients 2 and 4) mutations, indicating that the genotypic profile of collagen VI

genes alone may not be predictive of the disease phenotype. These findings suggest that mitochondria are involved in the pathogenesis of all cases of UCMD and that additional genetic and/or environmental factors play a role in the individual susceptibility to muscle fiber demise and regeneration. Consistent with this, the mouse model produced by targeted disruption of the *Col6a1* gene displays a complete absence of collagen VI, yet the phenotype resembles more the milder Bethlem myopathy than UCMD (11). This observation indicates that in the mouse model compensatory mechanisms may limit the net loss of muscle fibers and that similar mechanisms may be present to a variable degree in patients with collagen VI disorders. It should be noted that, together with the decreased levels of endomysial collagen VI, the anomalous response to oligomycin could represent a useful diagnostic tool for patients whose genetic lesion is undefined, as shown in this work for patient 3.

The trophic signals relayed from collagen VI to mitochondria remain elusive, although a prominent role for intracellular Ca^{2+} can be inferred both from studies in the mouse model (12) and from the effects of the intracellular Ca^{2+} chelator in the myoblasts from the UCMD patients. Moreover, lack of collagen VI caused a marked decrease of the BCL-2/BAX ratio attributable to decreased BCL-2 expression (data not shown). This decreased expression may synergize with Ca^{2+} in increasing the PTP open time (21), causing the release of cytochrome *c* and activation of caspase 3. Irrespective of the details of the mechanism, however, it is reassuring that the mitochondrial defects and ensuing apoptosis are normalized by cyclophilin inhibitors. Thus, the pathogenic chain of events downstream of the collagen VI genetic lesion can be interrupted by proper drugs, at least in the early stages, an observation that has tremendous potential for therapy. Indeed, disease progression depends on the balance between cell death and regeneration, and decreasing the rate of cell death by even a small factor may lead to a substantial improvement in the clinical course of the disease. We are also confident that the identification of the signaling pathways engaged by collagen VI upstream of mitochondria will offer additional targets and increase the chances of an effective therapy.

Besides its mitochondrial effects, CsA is well known to cause immunosuppression through the inhibition of calcineurin (22), which could be a major drawback in long-term treatment of patients. A key observation made here is that Debio 025, a specific cyclophilin inhibitor that desensitizes the PTP through mitochondrial cyclophilin D but has no inhibitory effects on calcineurin (16), is as effective as CsA at normalizing mitochondrial function and apoptotic rates in UCMD cells. This finding demonstrates that calcineurin is not involved in the cytoprotective effects of CsA and leads to perspectives on the pharmacological treatment of patients affected by collagen VI disorders.

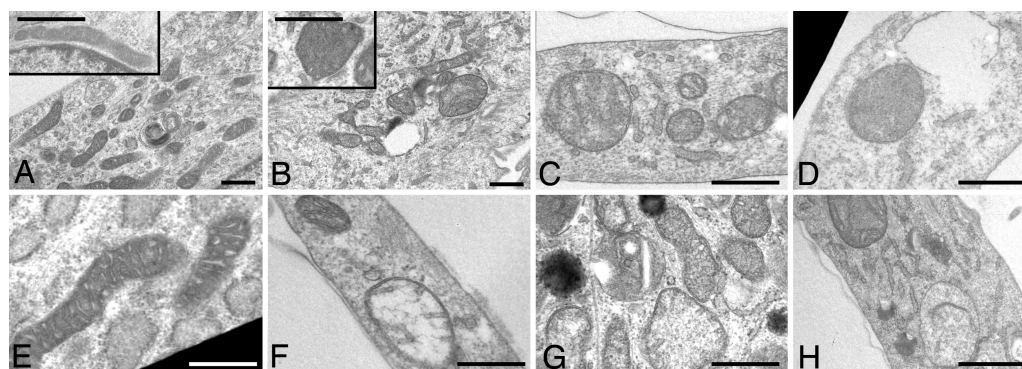


Fig. 4. Mitochondrial ultrastructure in muscle cell cultures from healthy donors and UCMD patients. (A–E) Electron micrographs of myoblasts from a healthy donor (A) and UCMD patients 1, 2, and 3 (B, C, and D, respectively) plated on plastic or on collagen VI (patient 2, E). (A and B insets) Higher magnifications from the same samples. (F–H) Representative examples of swollen mitochondria found in the myoblasts of patients 1 (F), 2 (G), and 3 (H). For further details and for a morphometric analysis see *Results*. (Scale bars, 300 nm.)

rameric collagen VI molecules ($5 \mu\text{g} \times \text{cm}^2$), previously purified from adult murine tissues as described (25).

Electron Microscopy. Cultures were washed with PBS, fixed with 2.5% glutaraldehyde in 0.1 M phosphate buffer (pH 7.4) and postfixed with 1% osmium tetroxide in veronal buffer. All samples were detached from the plastic dish with propylene oxide, centrifuged, and embedded in Epon E812 resin. Ultrathin sections were stained with uranyl acetate and lead citrate and observed with a Philips (Eindhoven, the Netherlands) EM400 electron microscope at 100 kV. For morphometric analysis, micrographs were taken at $\times 17,000$ magnification, and the area, perimeter, and short axis of mitochondria were determined by using the AnalySIS program (Soft Imaging System, Muenster, Germany). Three hundred cells were examined for each sample. For determination of area, perimeter, and short axis, cells with swollen mitochondria and necrotic aspects were not considered.

Detection of Proteins by Fluorescence Microscopy. Unfixed frozen sections of muscle biopsies from patients and from controls were double-labeled with mouse anti-collagen type VI (MAB 1944, 1:200 dilution; Chemicon, Temecula, CA) and rat anti-perlecan antibodies (1:100 dilution; Chemicon) for 1 h at room temperature in PBS containing 2% BSA, followed by fluorescein isothiocyanate-conjugated anti-mouse (Dako, Glostrup, Denmark), and tetramethylrhodamine isothiocyanate-conjugated anti-rat antibodies (Sigma). All samples were mounted with ProLong Antifade reagent (Molecular Probes, Carlsbad, CA) and observed with a Nikon (Tokyo, Japan) E600 fluorescence microscope. Cultured myoblasts from patients and controls were grown to confluence on coverslips and were treated with 0.25 M ascorbic acid for 5 days, to allow collagen molecules to be hydroxylated and secreted. Samples were fixed with cold methanol at -20°C for 7 min and incubated with anti-collagen VI (MAB 1944, 1:100 dilution; Chemicon) overnight at 4°C , followed by incubation with fluorescein isothiocyanate-conjugated anti-mouse antibodies (Dako).

Detection of Apoptosis. We measured the rate of apoptosis in muscle biopsies and in myoblast cultures using the terminal deoxynucleotidyltransferase-mediated dUTP nick end labeling (TUNEL) method. Frozen sections ($7 \mu\text{m}$ thick) were prepared from muscle biopsies of an unaffected control and five UCMD patients and fixed in 50% acetone/50% methanol. TUNEL was performed by using the ApopTag *in Situ* Apoptosis Detection kit (Chemicon). Samples were stained with peroxidase/diaminobenzidine to reveal TUNEL-positive nuclei. Myoblast cultures were seeded onto Lab-Tek plastic chamber slides (Nunc, Roskilde, Denmark) and grown to confluence in DMEM supplemented with 20% FCS. Cells were fixed in

50% acetone/50% methanol and processed for TUNEL analysis by using the DeadEnd Fluorometric TUNEL System (Promega, Madison, WI). Visualization of all nuclei was performed by staining with Hoechst 33258 (Sigma). The number of total and TUNEL-positive nuclei was determined in randomly selected fields by using a Zeiss (Oberkochen, Germany) Axioplan microscope ($\times 40$ magnification) equipped with a digital camera. Data are expressed as mean \pm SD. Data were analyzed with the unpaired Student's *t* test, and values of $P < 0.01$ were considered significant.

Mitochondrial Membrane Potential. This was measured based on the accumulation of tetramethylrhodamine methyl ester (TMRM). Myoblasts were seeded onto 24-mm-diameter round glass coverslips and grown for 2 days in DMEM supplemented with 20% FCS. The extent of cell and, hence, mitochondrial loading with potentiometric probes is affected by the activity of the plasma membrane multidrug resistance pump, which is inhibited by CsA. Treatment with this drug may therefore cause an increased mitochondrial fluorescence that can be erroneously interpreted as an increase of the mitochondrial membrane potential (26). To prevent this artifact and to normalize the loading conditions, in all experiments with TMRM the medium was supplemented with $1.6 \mu\text{M}$ CsH, which inhibits the multidrug resistance pump but not the PTP (27). Cells were rinsed once and then incubated in serum-free DMEM supplemented with $1.6 \mu\text{M}$ CsH and loaded with 10 nM TMRM for 30 min. At the end of each experiment, mitochondria were fully depolarized by the addition of $4 \mu\text{M}$ of the protonophore carbonyl cyanide *p*-trifluoromethoxyphenylhydrazone (FCCP). Cellular fluorescence images were acquired with an Olympus (Center Valley, PA) IX71/IX51 inverted microscope equipped with a xenon light source (75 W) for epifluorescence illumination and with a 12-bit digital cooled charge-coupled device (CCD) camera (Micromax, Princeton Instruments, Trenton, NJ). For detection of fluorescence, 568 ± 25 -nm bandpass excitation and 585-nm longpass emission filter settings were used. Images were collected with an exposure time of 100 msec by using a $\times 40$, 1.3 N.A. oil immersion objective (Nikon). Data were acquired and analyzed by using Cell^R software (Olympus). Clusters of several mitochondria (10–30) were identified as regions of interest, and fields not containing cells were taken as the background. Sequential digital images were acquired every 2 min, and the average fluorescence intensity of all relevant regions was recorded and stored for subsequent analysis.

We thank all individuals from the families who participated in this study and Debiopharm (Lausanne, Switzerland) for providing Debio 025. This study was supported by Telethon Italy Grant GGP04113, the Fondazione Carisbo, Association Française contre les Myopathies Grant 9398, and the Progetti di Ricerca di Interesse Nazionale of the Ministero dell'Università e della Ricerca (MIUR-PRIN).

- Lampe AK, Bushby KM (2005) *J Med Genet* 42:673–685.
- Bethlem J, Wijngaarden GK (1976) *Brain* 99:91–100.
- Merlini L, Morandi L, Granata C, Ballestrazzi A (1994) *Neuromuscul Disord* 4:503–511.
- Pepe G, Giusti B, Bertini E, Brunelli T, Saitta B, Comeglio P, Bolognese A, Merlini L, Federici G, Abbate R, et al. (1999) *Biochem Biophys Res Commun* 258:802–807.
- de Visser M, de Voogt WG, la Riviere GV (1992) *Muscle Nerve* 15:591–596.
- Ullrich O (1930) *Z Ges Neurol Psychiatr* 126:171–201.
- Camacho Vanegas O, Bertini E, Zhang RZ, Petrini S, Minosse C, Sabatelli P, Giusti B, Chu ML, Pepe G (2001) *Proc Natl Acad Sci USA* 98:7516–7521.
- Pan TC, Zhang RZ, Sudano DG, Marie SK, Bonnemann CG, Chu ML (2003) *Am J Hum Genet* 73:355–369.
- Baker NL, Morgelin M, Peat R, Goemans N, North KN, Bateman JF, Lamande SR (2005) *Hum Mol Genet* 14:279–293.
- Demir E, Sabatelli P, Allaman V, Ferreira A, Moghadaszadeh B, Makrelouf M, Topaloglu H, Echenne B, Merlini L, Guicheney P (2002) *Am J Hum Genet* 70:1446–1458.
- Bonaldo P, Braghetta P, Zanetti M, Piccolo S, Volpin D, Bressan GM (1998) *Hum Mol Genet* 7:2135–2140.
- Irwin WA, Bergamin N, Sabatelli P, Reggiani C, Megighian A, Merlini L, Braghetta P, Columbaro M, Volpin D, Bressan GM, et al. (2003) *Nat Genet* 35:267–271.
- Bernardi P, Krauskopf A, Basso E, Petronilli V, Blachly-Dyson E, Di Lisa F, Forte MA (2006) *FEBS J* 273:2077–2099.
- Giusti B, Lucarini L, Pietroni V, Luciosi S, Bandinelli B, Sabatelli P, Squarzone S, Petrini S, Gartioux C, Talim B, et al. (2005) *Ann Neurol* 58:400–410.
- Liu J, Farmer JDJ, Lane WS, Friedman J, Weissman I, Schreiber SL (1991) *Cell* 66:807–815.
- Hansson MJ, Mattiasson G, Mansson R, Karlsson J, Keep MF, Waldmeier P, Ruegg UT, Dumont JM, Besseghir K, Elmer E (2004) *J Bioenerg Biomembr* 36:407–413.
- Mitchell P (1979) *Science* 206:1148–1159.
- Vinogradov A, Scarpa A, Chance B (1972) *Arch Biochem Biophys* 152:646–654.
- Di Lisa F, Menabò R, Canton M, Barile M, Bernardi P (2001) *J Biol Chem* 276:2571–2575.
- Scorrano L, Ashiya M, Buttle K, Weiler S, Oakes SA, Mannella CA, Korsmeyer SJ (2002) *Dev Cell* 2:55–67.
- Milanesi E, Costantini P, Gambalunga A, Colonna R, Petronilli V, Cabrelle A, Semenzato G, Cesura AM, Pinard E, Bernardi P (2006) *J Biol Chem* 281:10066–10072.
- Clipstone NA, Crabtree GR (1992) *Nature* 357:695–697.
- Pepe G, Bertini E, Bonaldo P, Bushby K, Giusti B, de Visser M, Guicheney P, Lattanzi G, Merlini L, Muntoni F, et al. (2002) *Neuromuscul Disord* 12:984–993.
- Cenni V, Sabatelli P, Mattioli E, Marmiroli S, Capanni C, Ognibene A, Squarzone S, Maraldi NM, Bonne G, Columbaro M, et al. (2005) *J Med Genet* 42:214–220.
- Sabatelli P, Bonaldo P, Lattanzi G, Braghetta P, Bergamin N, Capanni C, Mattioli E, Columbaro M, Ognibene A, Pepe G, et al. (2001) *Matrix Biol* 20:475–486.
- Bernardi P, Scorrano L, Colonna R, Petronilli V, Di Lisa F (1999) *Eur J Biochem* 264:687–701.
- Nicolli A, Basso E, Petronilli V, Wenger RM, Bernardi P (1996) *J Biol Chem* 271:2185–2192.